Constructing the Universe with Clusters of Galaxies, IAP 2000 meeting, Paris (France) July 2000
Florence Durret & Daniel Gerbal eds.

THE ROSAT DEEP CLUSTER SURVEY: EVOLUTION OF THE LUMINOSITY FUNCTION OUT TO $z \simeq 1.3$


S. Borgani[1] & P. Rosati[2]
[1] *INFN - c/o Dipartimento di Astronomia dell'Università, Trieste, Italy*
[2] *ESO - European Southern Observatory, Garching, Germany*

1 Introduction

The number density of galaxy clusters has been recognized since ten years as a powerful cosmological test (e.g., Borgani et al. [1]; Henry [2], and references therein). Their abundance in the local Universe and the corresponding redshift evolution provide strong constraints on the amplitude of cosmic density perturbations on scales of about $10h^{-1}$ Mpc (h is the Hubble constant in units of 100 km s^{-1}Mpc^{-1}) and on the matter density parameter Ω_m.

Over the last five years, remarkable observational progress has been made in constructing large samples of local and distant galaxy clusters with the aim of quantifying the evolution of their space density and providing the basis for follow-up studies of their physical properties. The ROSAT satellite is largely responsible for this progress, both with All-Sky Survey data and pointed observations, which have been a gold mine for serendipitous discoveries.

About a thousand clusters have now been selected from the ROSAT All-Sky Survey and several statistical complete subsamples have been used to obtain a firm measurement of the local abundance of clusters [3,4]. Serendipitous searches for distant clusters, selected as extended X-ray sources in deep PSPC pointings [5,6,7,8], have boosted the number of known clusters at $z > 0.5$ by an order of magnitude, being just a few before the ROSAT era. This recent work has complemented the original Einstein Medium Sensitivity Survey (EMSS) [9,10], and has corroborated its findings.

In this paper, we report the most recent results from the ROSAT Deep Cluster Survey (RDCS) which has allowed these studies to be pushed beyond $z = 1$ for the first time [11]. After describing results about the evolution of the X–ray luminosity function, we show its cosmological implications on the determination of σ_8, the r.m.s. density fluctuation on 8 h^{-1} Mpc scale, and Ω_m. A more detailed description of our analysis will be presented in two forthcoming papers (Rosati et al. in preparation; Borgani et al. in preparation).

Unless otherwise stated, we assume $H_0 = 50$ km s^{-1} Mpc^{-1}.

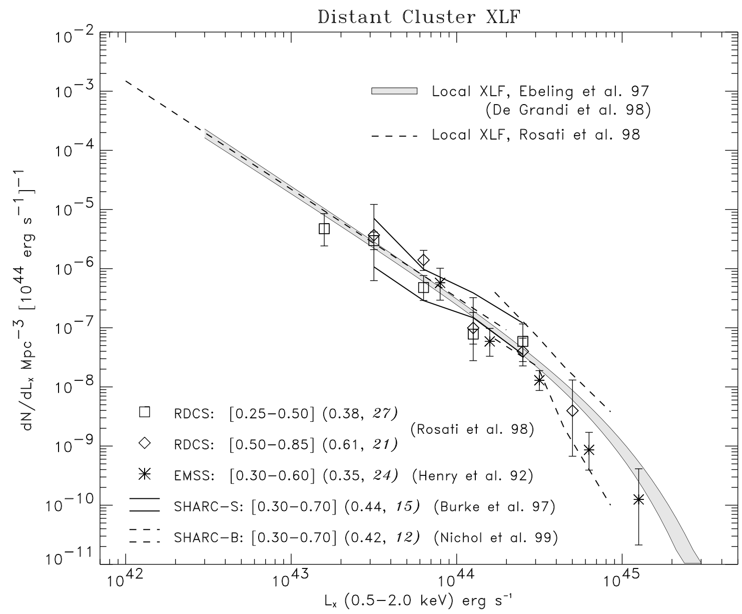

Figure 1: Distant and local cluster XLFs from the literature. The number in parenthesis are the median redshift and the number of clusters of various samples in each redshift bin.

2 The Evolution of the Cluster X-ray Luminosity Function

ROSAT distant cluster surveys [5,6,7,8], besides employing different X-ray selection methods, have adopted different strategies in terms of survey depth and solid angle. In Fig. 1 we show some measurements of the cluster XLF that have been published to date. Sample sizes and median redshifts of each sample are also indicated. Based on these data, several groups have argued that no significant evolution is observed in the space density of distant clusters with $L_X[0.5-2] \lesssim 3\times 10^{44}\,\mathrm{erg\,s^{-1}}$ [6,5,7,8]. As demonstrated by the RDCS[5], this trend persists out to $z\approx 0.8$. Measurements of the distant XLF at $L_X \gtrsim L_0^* \simeq 5\times 10^{44}\,\mathrm{erg\,s^{-1}}$ are difficult with current samples, due to low number statistics. As a result, the evolution of the high end of the XLF has remained a hotly debated issue, ever since it was first reported in the EMSS [9,10]. More recently, Vikhlinin et al. [8] have confirmed the EMSS findings by comparing the observed number of very luminous systems with the no evolution prediction. This result seems to be also in agreement with a preliminary analysis of the Bright SHARC sample [12] (Fig. 1).

The binned representation of the XLF in Fig.1 does not provide a full picture of the space density evolution observed in a given sample. For example, it fails to provide the statistical significance of a possible departure from no evolution models [13]. The information contained in the RDCS can be more readily recovered by analyzing the unbinned (L_X, z) distribution with a maximum-likelihood (ML) approach, which compares the observed cluster distribution on the (L_X, z) plane with that expected from a given XLF model.

We characterize the cluster XLF as an evolving Schechter function, $\phi(L)=\phi_0(1+z)^A L^{-\alpha}\exp(-L/L^*)$, with $L^*=L_0^*(1+z)^B$; where A and B are two evolutionary parameters. Different surveys find consistent values for the faint end slope α, which is not observed to vary as a function of redshift (Fig. 1). For the local XLF, we use here the measurement of the BCS sample [3], i.e. $\alpha=1.85$, $L_0^*=5.7\times10^{44}\,\mathrm{erg\,s^{-1}}$, $\phi_0=3.32\,(10^{-7}\mathrm{Mpc^{-3}L_{44}^{\alpha-1}})$.

For this analysis, we use a complete flux limited sample ($F_{lim}=3.5\times10^{-14}$ erg cm^{-2} s^{-1}) of 81 spectroscopically confirmed RDCS clusters drawn from 33 deg^2 ($z_{\max}=0.83$, Rosati et al. in preparation). Observed flux errors are included in the likelihood computation. The resulting 1σ, 2σ and 3σ c.l. contours in the A-B plane are shown in Fig. 2, for two different cosmologies.

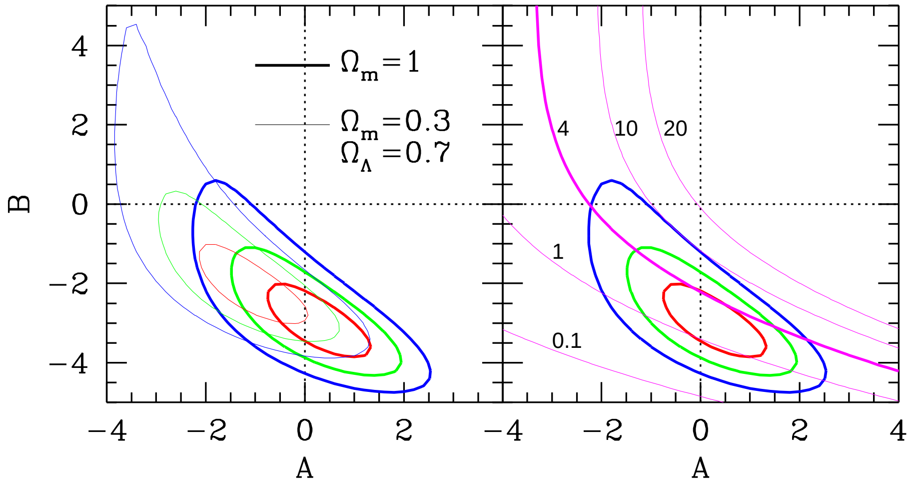

Figure 2: *Left:* Confidence regions in the plane of the two evolutionary parameters A and B obtained by fitting the function $\phi(L) = \phi_0(1+z)^A L^{-\alpha} \exp(-L/L^*)$, $L^* = L_0^*(1+z)^B$, to an RDCS subsample. Maximum likelihood contours (1σ, 2σ and 3σ confidence levels) are plotted for two different cosmologies. *Right*: Loci of the A-B plane for which the corresponding XLF predicts 0.1, 1, 4, 10, 20 clusters at $z > 1$ for the whole RDCS sample ($F_{lim} = 1 \times 10^{-14}\,\mathrm{erg\,s^{-1}cm^{-2}}$). The RDCS includes 4 spectroscopically confimed clusters at $z > 1$to date.

Best fit values for the $\Omega_m = 1$ case are

$$A = 0.4^{+1.5}_{-1.8} \qquad ; \qquad B = -3.0^{+1.8}_{-1.2} \tag{1}$$

where errors correspond to the 2σ c.l. for two significant fitting parameters. The no evolution model ($A = B = 0$) is excluded at more than a 3σ confidence level, even when the uncertainties of the local XLF are taken into account. The departure of our best fit model from the no-evolution scenario is due to the small number of observed clusters in the RDCS at $z >0.5$ with luminosities $L_X \gtrsim L_0^*$ compared to the no-evolution prediction. Interestingly, this effect is barely significant with a slightly shallower sample ($F_{lim} = 4 \times 10^{-14}\,\mathrm{erg\,s^{-1}cm^{-2}}$, 70 clusters). This evolutionary trend is similar to that observed in the EMSS [10,9].

By excluding the most luminous clusters from our ML analysis, we find that there is *no evidence of evolution* (with 2σ confidence level) at luminosities $L_X \lesssim 2\times10^{44}\,\mathrm{erg\,s^{-1}}$, confirming previous results obtained with smaller samples. A redshift dependent inspection of the likelihood also shows that little can be said on the evolution of the high end of the XLF at $z \lesssim 0.5$ with the current RDCS sample.

These findings lead to a consistent picture in which the comoving space density of the bulk of the cluster population is approximately constant out to $z \sim 0.8$, but the most luminous ($L_X \gtrsim L_0^*$), presumably most massive clusters were indeed rarer at high redshifts.

3 Constraints on cosmological models

Having quantified the degree of evolution of the cluster XLF, it is worth asking which are its implications on the determination of cosmological parameters. To this purpose, we rely on the Press-Schechter approach as the starting point for computing the cluster mass function predicted by a given cosmological model. As shown by Borgani et al. [1], it provides a good description of the cluster mass distribution in the range probed by RDCS. The conversion from masses to X-ray luminosities, which is required to convert a mass function into a XLF, is implemented as follows: **(a)** convert mass into temperature by assuming virialization, hydrostatic equilibrium

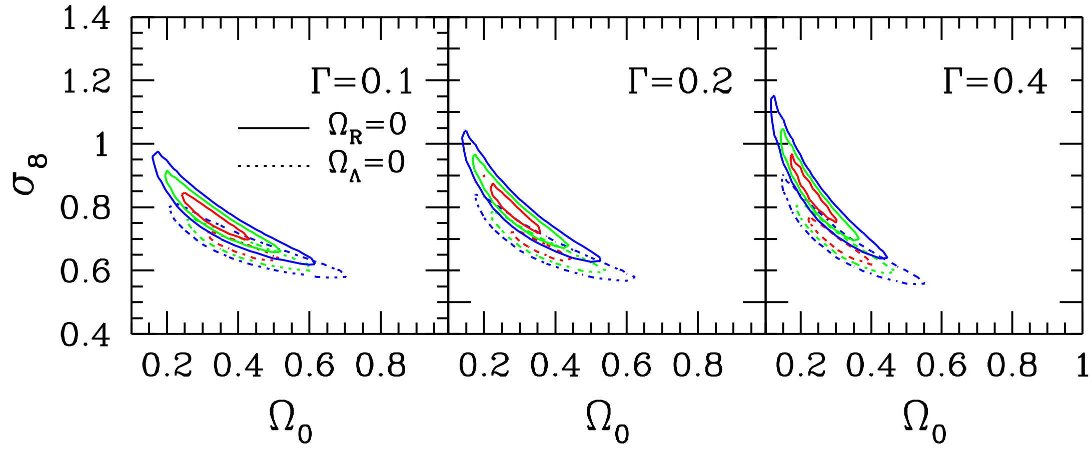

Figure 3: Confidence regions on the Ω_m–σ_8 plane. In all the panels, solid contours and dashed contours are for flat and open models, respectively. Here $\alpha = 3.5$, $A = 0$ and $\beta = 1.15$ are assumed for the mass–luminosity conversion. Contours are 1σ, 2σ and 3σ c.l. for two significant parameters.

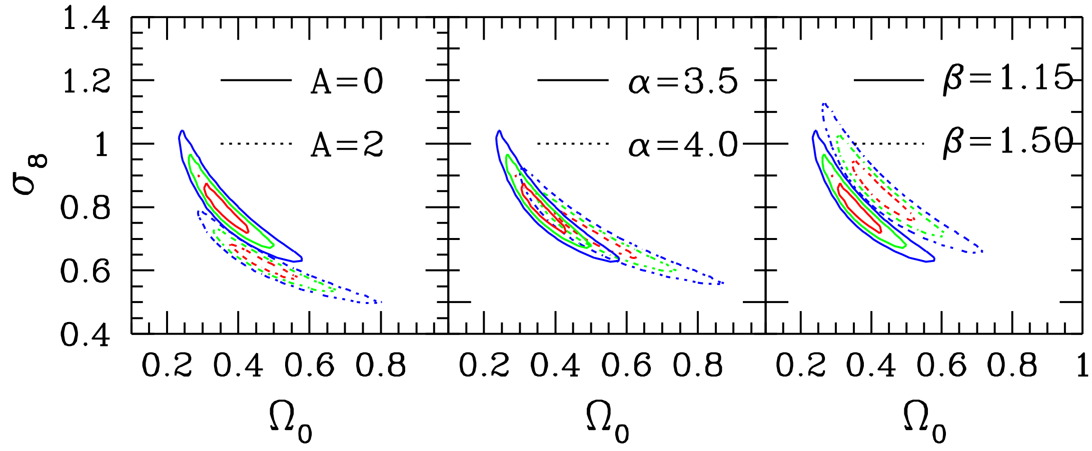

Figure 4: Effect of changing the L_{bol}–T_X relation. Solid contours are from assuming $\Gamma = 0.2$, $\alpha = 3.5$, $A = 0$ and $\beta = 1.15$. Contours have the same meaning as in Fig. 3.

and isothermal gas distribution; **(b)** convert temperature into bolometric luminosity according to $L_{bol} \propto T^\alpha (1+z)^A$; **(c)** compute the bolometric correction to the 0.5-2.0 keV band.

The critical step is represented by the choice for the L_{bol}–T_X relation. Low redshift data for $T \gtrsim 3\,\mathrm{keV}$ indicates that $\alpha \simeq 2.7$–3.5, depending on the sample and the data analysis technique [14], with a reduction of the scatter after account for the effect of cooling flows in central cluster regions [15]. At lower temperatures, evidence has been found for a steepening of the L_{bol}–T_X relation below 1 keV [16]. As for the evolution of the L_{bol}–T_X relation, existent data out to $z \simeq 0.4$ [17] and, possibly, out to $z \sim 0.8$ [18] are consistent with no evolution (i.e., $A \simeq 0$). Instead of assuming a unique mass–luminosity conversion, in the following we will show how final constraints on cosmological parameters changes as the L_{bol}–T_X and M–T_X relations are varied.

In order to fully exploit the information provided by the RDCS, we resort again to a maximum–likelihood approach, in which model predictions are compared to the RDCS cluster distribution on the (L, z) plane.

Model predictions are convolved with statistical errors on measured fluxes, as well as with uncertainties in the luminosity–mass relation associated to a $\simeq$ 30% scatter in the L_{bol}–T_X relation and to a 20% uncertainty in the mass–temperature conversion.

In Figure 3 we show the resulting constraints on the σ_8–Ω_m plane for different values of the shape parameter Γ, based on assuming $\alpha = 3.5$ and $A = 0$ for the L_{bol}–T_X relation. It is clear that low–density models are always preferred, quite independent of Γ. We find

$$\begin{aligned} \Omega_m &= 0.35^{+0.35}_{-0.25} \quad ; \quad \sigma_8 = 0.76^{+0.38}_{-0.14} \qquad (\Omega_\Lambda = 1 - \Omega_m) \\ \Omega_m &= 0.42^{+0.35}_{-0.27} \quad ; \quad \sigma_8 = 0.68^{+0.21}_{-0.12} \qquad (\Omega_\Lambda = 0) \end{aligned} \tag{2}$$

where uncertainties correspond to 3σ confidence level for three significant fitting parameter. No significant constraints are instead found for Γ. In order to verify under which circumstances a critical density model may still be viable, we show in Figure 4 the effect of changing the parameters of the L_{bol}–T_X relation. Although best–fitting values of Ω_m and σ_8 move somewhat on the parameter space, neither a rather strong evolution nor a quite steep profile for the L_{bol}–T_X relation can accommodate a critical density Universe: an $\Omega_m = 1$ Universe is always a $> 3\sigma$ event, even allowing for values of the A and α parameters which are strongly disfavored by present data.

Based on these results, we point out that deep flux–limited X–ray cluster samples, like RDCS, which cover a large redshift baseline ($0.1 \lesssim z \lesssim 1.2$) and include a fairly large number of clusters ($\gtrsim 100$) do indeed place significant constraints on cosmological models. To this aim, some knowledge of the L_{bol}–T_X evolution is needed from a (not necessarily complete) sample of distant clusters out to $z \sim 1$.

4 Future perspectives

The next obvious step in the effort to understand cluster formation and evolution is to push the cluster (or proto-cluster) search out to even higher redshifts, namely out to $z \sim 3$ where the signature of large scale structure has already been unveiled [19]. Finding clusters around high-z AGN is a viable method[20,21], although not suitable for assessing the cluster abundance. Serendipitous searches with Chandra and XMM will of course be actively pursued, but it will take several years to build large enough survey areas, and furthermore, the spectroscopic follow-up of cluster candidates at $z > 1.3$ may turn out to be too difficult with existing telescopes. While the short-term prospects for exploring the era at $1.5 \lesssim z \lesssim 2.5$ may appear somewhat bleak, it should be kept in mind that earlier this decade many theorists and observers were convinced that clusters at $z > 1$ were either out of reach, or did not exist.

From the viewpoint of using distant clusters for constraining cosmology, our analysis demonstrates that the main limitation is still represented by the partial knowledge of the ICM physics and, therefore, of the relation between the cluster mass and its X–ray emissivity. As more and higher quality data will be accumulated, thanks to the new generation of X–ray satellites, this limitation will be probably much reduced. This will open the possibility of using the number density of high–redshift clusters as a high–precision cosmological test, complementing those from measurements of CMB anisotropies.

References

1. Borgani, S., Rosati, P., Tozzi, P., & Norman, C. 1999, ApJ, 517, 40
2. Henry, J.P. 2000, ApJ, 534, 565
3. Ebeling, H., Edge, A.C., Fabian, A.C., Allen, S.W., Crawford, C.S., & Böhringer, H. 1997, ApJ, 479, L101
4. De Grandi, S., Böhringer,H., Guzzo, L., 1999, ApJ, 514, 148

5. Rosati, P., Della Ceca, R., Norman, C., & Giacconi, R. 1998, ApJ, 492, L21
6. Burke, D.J., Collins, C.A., Sharples, R.M., Romer, A.K., Holden, B.P., & Nichol, R.C. 1997, ApJ, 488, L83
7. Jones, L.R., Scharf, C., Ebeling, H., Perlman, E., Wegner, G., Malkan, M., & Horner, D. 1998, ApJ, 495, 100
8. Vikhlinin A., McNamara, B.R., Forman, W., Jones, C., Quintana, H., & Hornstrup, A. 1998, ApJ, 498, L21
9. Gioia, I.M., Henry, J.P., Maccacaro, T., Morris, S.L., Stocke, J.T., & Wolter, A. 1990, ApJ, 356, L35
10. Henry, J.P., Gioia, I.M., Maccacaro, T., Morris, S.L., Stocke, J.T., & Wolter, A. 1992, ApJ, 386, 408
11. Rosati, P., Stanford, S.A., Eisenhardt, P.R., Elston, R., Spinrad, H., Stern, D., & Dey, A. 1999, AJ, 118, 76
12. Nichol, R.C., Romer, A.K., Holden, B.P., et al. 1999, ApJ, 521, L21
13. Page, M.J., & Carrera, F.J. 2000, MNRAS, 311, 433
14. White, D.A., Jones, C., & Forman, W. 1997, MNRAS, 292, 419
15. Arnaud, K.A., & Evrard, A.E. 1999, MNRAS, 305, 631
16. Helsdon, S.F., & Ponman, T.J. 2000, MNRAS, 315, 356
17. Mushotzky, R.F., & Scharf, C.A. 1997, ApJ, 482, L13
18. Della Ceca, R., Scaramella, R., Gioia, I.M., Rosati, P., Fiore, F., & Squires, G.. 2000, A&A, 353, 498
19. Steidel C.C., Adelberger, K.L., Giavalisco, M., Dickinson, M., & Pettini, M. 1999, ApJ, 519, 1
20. Crawford, C.S. & Fabian, A.C. 1996, MNRAS, 282, 1483
21. Carilli, C.L., Harris, D.E., Pentericci, L., Rottergering, H.J.A., Miley, G.K., & Bremer, M.N. 1998, ApJ, 494, L143